Discussion Paper No.298

Delay Cournot Duopoly Models Revisited

Luca Guerrini
Polytechnic University of Marche

Akio Matsumoto
Chuo University

Ferenc Szidarovszky
University of Pécs

January 2018

Delay Cournot Duopoly Models Revisited[*]

Luca Guerrini[†] Akio Matsumoto[‡] Ferenc Szidarovszky[§]

Abstract

In considering economic dynamics, it has been known that time delays are inherent in economic phenomena and could be crucial sources for oscillatory behavior. The main aim of this study is to shed light on what effects the delays can generate. To this end, three different models of Cournot duopoly with different delays are build in a continuous time framework and their local and global dynamics are analytically and numerically examined. Three major findings are obtained. First, the stability switching conditions are analytically constructed. Second, it is numerically demonstrated that different length of the delays are sources for the birth of simple and complicated dynamics. Third, the delay for collecting information on the competitors' output alone does not affect stability.

Keywords: Implementation delay, Information delay, Cournot duopoly, Stability switching curve, Dual roles, Bifurcation diagram

In competitive markets the firms make their optimal decisions based on those of the competitors. However this information is not instantaneous because of delays in data collection, in determining optimal decisions and also in their implementation. These delays have significant effects in the long-term behavior of the associated dynamic systems. This paper investigates this effect in cases of duopolies when only two competing firms are present. Three particular models are examined, in which the equilibrium is locally asymptotically stable without delays. In the first model both information and implementation delays are assumed and it is shown that the delays have the dual rules of destabilizing and stabilizing the equilibrium involving chaotic behavior with larger values of the delays. In the second model only information delays are assumed on the competitors' outputs and it is verified that the delays have no effect on the stability of the equilibrium. In the third model only implementation delays are assumed which can destabilize the otherwise stable equilibrium without the dual rule. In addition to the theoretical developments computer studies illustrate and verify the theoretical findings.

1   Introduction

This paper reconsiders the stability conditions of the delay Cournot oligopoly models studied by Howroyd and Russel (1984) ("HR" henceforth). Constructing n-firm Cournot oligopoly models in a continuous-time framework, HR provides a sufficient condition for stability under circumstances in which each firm experiences delays in implementing information on its own output (i.e., implementation delay) and in collecting information on its competitors' outputs (i.e., information delay). Further, HR shows that the information delays do not affect stability when each firm has the information delay on its competitors' outputs but instantaneous knowledge on its own output. Based on these results, we move one step forward and investigate a sufficient and necessary condition for stability. To simplify the complicated problem, we draw attention only to a Cournot duopoly in this study.

Oligopoly theory has a long history since the pioneering work of Cournot (1883). Its stability properties are first investigated by Theocharis (1960). It is shown that only the number of the firms involved in a market determines stability of a linear Cournot oligopoly in a discrete-time framework: the steady state is stable in the duopoly, marginal stable in the triopoly and unstable if the number is more than three. McManus and Quandt (1961) and Hahn (1962) prove asymptotically stability in the continuous-time adjustment process with demand and cost functions having the appropriate slopes. Okuguchi (1976) summarizes the early results on static and dynamic oligopolies. Okuguchi and Szidarovszky (1999) discuss their multiproduct generalization. During the last two decades, an increasing attention has been given mainly to discrete-time nonlinear dynamics. Bischi et al. (2010) give a comprehensive summary of the newer developments. As the same as an ordinary differential equation, the stability of a delay differential equation depends on the location of the roots of the associated characteristic equation. In consequence, the roots are functions of delays and thus the stability may change as the length of delay changes. Such phenomena are referred to as *stability switches*. For differential equations with one delay, Cooke and Grossman (1982) improve the key techniques to utilize. However, concerning multi-delay dynamics, it has not been discussed until quite recently. This is because the inclusion of multiple delays in equations makes the detail descriptions of the dynamic process too complicated and in addition, no mathematical methods are available for dealing with such delay dynamic models, although importance of multiple delays inherent in the process of obtaining information has been realized. Only recently, Gu et al. (2005) and Lin and Wang (2012) independently develop the useful procedures to construct the stability switching curves for dif-

ferential equations with multiple delays. With these curves, it can be detected under which the delay systems lose or gain stability. See Matsumoto and Szidarovszky (2015) and Gori et al. (2015) that adopt the methods for analyzing delay dynamics of Cournot duopoly.

In this paper, we present three different Cournot duopoly models with multiple delays, the first model includes both of the implementation and information delays, the second model possesses only the information delays and the third model is endowed with only the implementation delays. Applying the Lin-Wang method, we analytically and numerically investigate stability of these models and find that the delay models may explain various dynamics ranging from simple to complex behavior under Cournot competition.

This paper is organized as follows. Section 2 is divided into two subsections. In the first, we build a delay duopoly model based on HR's n-firm Cournot model and present a stability condition. In the second, we specify the parameter values and illustrate the stability switching curve under identical parameter condition. In Section 3, we focus on the special case where the firms have only information delays and confirm the corresponding HR result. In Section 4, we turn attention to a case where the firms have only implementation delays, the case which HR does not consider. In Section 5, we numerically examine how the stability properties change when certain nonlinearities are introduced into the adjustment process and the identical conditions are taken away. In the final section, concluding remarks and further research directions are given.

2 Delay Duopoly Model I

2.1 Duopoly Version of the Howroyd and Russel Model

Constructing a Cournot profit maximizing model in which n firms have linear price and quadratic cost functions, HR derives a linear best reply function of firm i as

$$x_i^* = \alpha_i - \beta_i \sum_{j \neq i} x_j \text{ for } i, \ j = 1, 2, ...n \tag{1}$$

where α_i and β_i are positive constants and x_j is output of firm j. Concerning the continuous-time adjustment of output, it is assumed that firm i adjusts its output at a rate proportional to the difference between its best reply output and its actual output at some proceeding time $t - \tau_i$,

$$\frac{dx_i}{dt} = k_i \left[x_i^*(t - \tau_i) - x_i(t - \tau_i) \right] \text{ for } i = 1, 2, ..., n \tag{2}$$

where $\tau_i \geq 0$ denotes a delay and $k_i > 0$ is the adjustment coefficient. After determining Cournot equilibrium output x_i^e as the solution of equations

$$x_i^e + \beta_i \sum_{j \neq i} x_j^e = \alpha_i \text{ for } i, j = 1, 2, ..., n$$

HR provides a **sufficient condition** for stability of the equilibrium point,

$$\tau_i \leq \frac{1}{2k_i} \text{ for } i = 1, 2, ...n \tag{3}$$

under the parametric assumption

$$(n - 1)\beta_i < 1.$$

In this study, we confirm a sufficient and necessary condition for stability of the various versions of the delay HR model in the duopoly framework (i.e., $n = 2$) in which the equilibrium outputs

3

are explicitly obtained,

$$x_1^e = \frac{\alpha_1 - \alpha_2 \beta_1}{1 - \beta_1 \beta_2} \text{ and } x_2^e = \frac{\alpha_2 - \alpha_1 \beta_2}{1 - \beta_1 \beta_2}.$$

To avoid negative output, we impose the following conditions on the parameters.

Assumption 1. $\beta_i < 1$ for $i = 1, 2$ and $\beta_2 \leq \dfrac{\alpha_2}{\alpha_1} \leq \dfrac{1}{\beta_1}$.

For stability analysis, we substitute the best replies into the delay differential equation (2) and then consider its homogenous system with multiple delays $\tau_1 \geq 0$ and $\tau_2 \geq 0$,

$$\frac{dx_1}{dt} = k_1 \left[-x_1(t - \tau_1) - \beta_1 x_2(t - \tau_1) \right],$$

$$\frac{dx_2}{dt} = k_2 \left[-\beta_2 x_1(t - \tau_2) - x_2(t - \tau_2) \right]. \tag{4}$$

With an exponential solution for the form

$$x_i = e^{\lambda t} \xi_i,$$

the characteristic equation of (4) is derived as

$$\det \begin{pmatrix} \lambda + k_1 e^{-\lambda \tau_1} & k_1 \beta_1 e^{-\lambda \tau_1} \\ k_2 \beta_2 e^{-\lambda \tau_2} & \lambda + k_2 e^{-\lambda \tau_2} \end{pmatrix} = 0$$

or

$$P_0(\lambda) + P_1(\lambda) e^{-\lambda \tau_1} + P_2(\lambda) e^{-\lambda \tau_2} + P_3(\lambda) e^{-\lambda(\tau_1 + \tau_2)} = 0 \tag{5}$$

where

$$P_0(\lambda) = \lambda^2, \ P_1(\lambda) = k_1 \lambda, \ P_2(\lambda) = k_2 \lambda, \ P_3(\lambda) = k_1 k_2 (1 - \beta_1 \beta_2).$$

If the characteristic equation (5) has roots only with the negative real parts, then the zero solution of delay system (4) is locally asymptotically stable. Thus our problem is to determine parametric conditions under which all roots of the characteristic equation lie in the left half of the complex plane.

If $\tau_1 = \tau_2 = 0$, then (5) becomes

$$\lambda^2 + (k_1 + k_2) \lambda + k_1 k_2 (1 - \beta_1 \beta_2) = 0$$

where the two roots of this equation are real and negative if $\beta_1 < 1$ and $\beta_2 < 1$. Hence Assumption 1 guarantees stability of the stationary point of the duopoly model with no-delay. We now suppose that $\tau_1 \geq 0$ and $\tau_2 \geq 0$ but not $\tau_1 = \tau_2 = 0$. It is assumed that (τ_1, τ_2) varies continuously in $R_+^2 = \{(\tau_1, \tau_2) \mid \tau_1 \geq 0 \text{ and } \tau_2 \geq 0)\}$. Since $\lambda = 0$ is not a root of (5), the number of eigenvalues having a positive real part can change only if an eigenvalue appears on or crosses the imaginary axis. Therefore in order to study stability, we need to find all pure complex roots of equation (5). We thus look for a pair of delays for which (5) has purely imaginary roots. Since roots of real function always come in conjugate pairs, it can be assumed, without loss of generality, that $\lambda = i\omega$ with $\omega > 0$. Substituting it into (5) presents the form

$$P_0(i\omega) + P_1(i\omega) e^{-i\omega \tau_1} + P_2(i\omega) e^{-i\omega \tau_2} + P_3(i\omega) e^{-i\omega(\tau_1 + \tau_2)} = 0 \tag{6}$$

with
$$P_0(i\omega) = -\omega^2, \; P_1(i\omega) = ik_1\omega, \; P_2(i\omega) = ik_2\omega, \; P_3(i\omega) = k_1k_2(1 - \beta_1\beta_2). \tag{7}$$

Applying the method developed by Lin and Wang (2012), we derive the set of (τ_1, τ_2) for which the delay dynamic system (4) loses stability. Equation (6) can be rewritten as

$$\left(P_0 + P_1 e^{-i\omega\tau_1}\right) + \left(P_2 + P_3 e^{-i\omega\tau_1}\right) e^{-i\omega\tau_2} = 0 \tag{8}$$

where the arguments of P_0, P_1, P_2 and P_3 are omitted for the sake of simplicity. Since $\left|e^{-i\omega\tau_2}\right| = 1$, equation (8) has solution for τ_1 if and only if

$$\left|P_0 + P_1 e^{-i\omega\tau_1}\right| = \left|P_2 + P_3 e^{-i\omega\tau_1}\right|$$

or equivalently,

$$\left(P_0 + P_1 e^{-i\omega\tau_1}\right)\left(\bar{P}_0 + \bar{P}_1 e^{i\omega\tau_1}\right) = \left(P_2 + P_3 e^{-i\omega\tau_1}\right)\left(\bar{P}_2 + \bar{P}_3 e^{i\omega\tau_1}\right),$$

where over-bar indicates complex conjugate. After some algebra, the last equation has the form

$$|P_0|^2 + |P_1|^2 - |P_2|^2 - |P_3|^2 = 2A_1\left(\omega\right)\cos\omega\tau_1 - 2B_1(\omega)\sin\omega\tau_1 \tag{9}$$

with

$$A_1\left(\omega\right) = \text{Re}\left(P_2\bar{P}_3 - P_0\bar{P}_1\right) \text{ and } B_1(\omega) = \text{Im}\left(P_2\bar{P}_3 - P_0\bar{P}_1\right).$$

The left hand side of equation (9) depends only on ω and the right hand side is a simple trigonometric equation for τ_1 with any fixed value of ω. Denoting the left hand side by $f(\omega)$, we first check the existence of solutions for equation (9).

Using (7), we can confirm that

$$P_2\bar{P}_3 - P_0\bar{P}_1 = ik_1\omega\left[k_2^2\left(1 - \beta_1\beta_2\right) - \omega^2\right]$$

implying that

$$A_1\left(\omega\right) = 0 \text{ and } B_1(\omega) = k_1\omega\left[k_2^2\left(1 - \beta_1\beta_2\right) - \omega^2\right].$$

We examine the case of $B_1(\omega) = 0$ and then the case of $B_1(\omega) \neq 0$ in the following.

Case I. $A_1\left(\omega\right) = B_1(\omega) = 0$

Let ω_0 be the positive solution of $B_1(\omega) = 0$,

$$\omega_0 = k_2\sqrt{1 - \beta_1\beta_2} > 0.$$

Substituting $P_j(i\omega)$ for $j = 0, 1, 2, 3$ defined in (7) into $f(\omega)$ gives

$$f(\omega) = \omega^4 + \left(k_1^2 - k_2^2\right)\omega^2 - \left(k_1k_2\right)^2\left(1 - \beta_1\beta_2\right)^2.$$

Then solving $f(\omega) = 0$ for ω^2 yields a positive solution

$$\omega_+^2 = \frac{-\left(k_1^2 - k_2^2\right) + \sqrt{\left(k_1^2 - k_2^2\right)^2 + 4\left(k_1k_2\right)^2\left(1 - \beta_1\beta_2\right)^2}}{2} > 0$$

that is reduced to ω_0^2 if $k_1 = k_2$ and not equal to it if $k_1 \neq k_2$. We then have two possibilities. First, if $k_1 \neq k_2$, then $f(\omega) \neq 0$ for $\omega = \omega_0$. Thus there is no solution for τ_1 since equation (9) is contradiction. On the other hand, if $k_1 = k_2$, then $f(\omega) = 0$ for $\omega = \omega_0$. Thus $\tau_1 > 0$ is arbitrary, and the corresponding values of τ_2 can be obtained from equation (8) as

$$e^{-i\omega\tau_2} = -\frac{P_0(i\omega) + P_1(i\omega)e^{-i\omega\tau_1}}{P_2(i\omega) + P_3(i\omega)e^{-i\omega\tau_1}} \tag{10}$$

where the absolute value of the right hand side is unity for all values of τ_1. Therefore there are infinitely many solutions of τ_2 because of periodicity of trigonometric functions. A locus of τ_1 and τ_2 satisfying (10) is called a *crossing curve* on which roots of (6) cross the imaginary axis when τ_2 changes and τ_1 is fixed (or alternatively τ_1 changes and τ_2 is fixed). Since the zero solution of (4) is locally asymptotically stable with no delays and its stability depends on the lengths of the positive delays, there may be the curve on which the stability of the zero solution changes. We call such a curve a *stability switching curve*. The result obtained is summarized as follows:

Theorem 1 *If the adjustment coefficients of the two firms are identical (i.e., $k_1 = k_2$), then the crossing curve in Case I is described by $(\tau_1, \tau_2^\ell(\tau_1))$ where*

$$\tau_2^\ell(\tau_1) = \frac{1}{\omega_0}\left\{ \arg\left[-\frac{P_2(i\omega_0) + P_3(i\omega_0)e^{-i\omega_0\tau_1}}{P_0(i\omega_0) + P_1(i\omega_0)e^{-i\omega_0\tau_1}}\right] + 2\ell\pi \right\} \ \text{for} \ \ell = 0, \ \pm 1, \ \pm 2, ... \tag{11}$$

Case II. $[A_1(\omega)]^2 + [B_1(\omega)]^2 > 0$

We have already known that $A_1(\omega) = 0$ for any $\omega \geq 0$ and $B_1(\omega) \neq 0$ for $\omega \neq \omega_0$. There exists $\varphi_1(\omega)$ such that

$$\varphi_1(\omega) = \arg\left[P_2\bar{P}_3 - P_0\bar{P}_1\right] = \begin{cases} \dfrac{\pi}{2} & \text{if } B_1(\omega) > 0 \text{ or } \omega < \omega_0, \\[2mm] \dfrac{3\pi}{2} & \text{if } B_1(\omega) < 0 \text{ or } \omega > \omega_0, \end{cases}$$

implying that

$$\sin[\varphi_1(\omega)] = \frac{B_1(\omega)}{\sqrt{[B_1(\omega)]^2}} \ \text{and} \ \cos[\varphi_1(\omega)] = \frac{A_1(\omega)}{\sqrt{[B_1(\omega)]^2}} = 0.$$

Using these relations, Equation (9) is reduced to

$$|P_0|^2 + |P_1|^2 - |P_2|^2 - |P_3|^2 = 2\sqrt{[B_1(\omega)]^2}\cos(\varphi_1(\omega) + \omega\tau_1) \tag{12}$$

that can be rewritten as

$$\frac{|P_0|^2 + |P_1|^2 - |P_2|^2 - |P_3|^2}{2\sqrt{[B_1(\omega)]^2}} = \cos[\varphi_1(\omega) + \omega\tau_1].$$

A sufficient and necessary conditions for the existence of $\tau_1 \geq 0$ satisfying the above equation is

$$\left||P_0|^2 + |P_1|^2 - |P_2|^2 - |P_3|^2\right| \leq 2\sqrt{[B_1(\omega)]^2}$$

or

$$F(\omega) = \left[|P_0|^2 + |P_1|^2 - |P_2|^2 - |P_3|^2\right]^2 - 4[B_1(\omega)]^2 \leq 0.$$

6

With the notation of $x = \omega^2$, the right hand side of $F(\omega)$ is reduced to the following form and denoted as

$$g(x) = x^4 + a_3 x^3 + a_2 x^2 + a_1 x + a_0$$

where the coefficients are defined as

$$
\begin{aligned}
a_3 &= -2(k_1^2 + k_2^2), \\
a_2 &= (k_1^2 - k_2^2)^2 + 2(k_1 k_2)^2 (3 + \beta_1 \beta_2)(1 - \beta_1 \beta_2), \\
a_1 &= -2(k_1^2 + k_2^2)[k_1 k_2 (1 - \beta_1 \beta_2)]^2, \\
a_0 &= [k_1 k_2 (1 - \beta_1 \beta_2)]^4.
\end{aligned}
$$

Solving $g(x) = 0$ yields four real solutions,

$$x_1 = \frac{1}{2}\left[k_1^2 + k_2^2 - 2k_1 k_2 \beta_1 \beta_2 - (k_1 - k_2)\sqrt{d_1} \right],$$

$$x_2 = \frac{1}{2}\left[k_1^2 + k_2^2 - 2k_1 k_2 \beta_1 \beta_2 + (k_1 - k_2)\sqrt{d_1} \right],$$

$$x_3 = \frac{1}{2}\left[k_1^2 + k_2^2 + 2k_1 k_2 \beta_1 \beta_2 - (k_1 + k_2)\sqrt{d_2} \right],$$

$$x_4 = \frac{1}{2}\left[k_1^2 + k_2^2 + 2k_1 k_2 \beta_1 \beta_2 + (k_1 + k_2)\sqrt{d_2} \right],$$

where both discriminants are positive,

$$d_1 = (k_1 + k_2)^2 - 4k_1 k_2 \beta_1 \beta_2 > 0$$

and

$$d_2 = (k_1 - k_2)^2 + 4k_1 k_2 \beta_1 \beta_2 > 0.$$

Positive solutions of $x_i = \omega^2$ are denoted by ω_i where

$$\omega_3 < \omega_4 \text{ and } \omega_1 \gtreqless \omega_2 \text{ according to } k_1 \gtreqless k_2.$$

The interval $[\omega_3, \omega_i] \cup [\omega_j, \omega_4]$ is denoted by Ω in which $F(\omega) \leq 0$ and $\omega_i = \omega_1$ and $\omega_j = \omega_2$ if $k_1 > k_2$ and ω_i is interchanged with ω_j if the inequality is reversed.

Let us define $\psi_1(\omega)$ by

$$|P_0|^2 + |P_1|^2 - |P_2|^2 - |P_3|^2 = 2\sqrt{B(\omega)_1{}^2} \cos[\psi_1(\omega)]. \tag{13}$$

So

$$\psi_1(\omega) = \cos^{-1}\left[\frac{|P_0|^2 + |P_1|^2 - |P_2|^2 - |P_3|^2}{2\sqrt{B_1(\omega)^2}} \right].$$

Comparing the right hand side of (12) with that of (13) yields

$$\tau_{1,n}^{\pm}(\omega) = \frac{1}{\omega}\left[\pm \psi_1(\omega) - \varphi_1(\omega) + 2n\pi \right]. \tag{14}$$

Returning to (6), we can see that it can be alternatively put as

$$\left(P_0 + P_2 e^{-i\omega\tau_2} \right) + \left(P_1 + P_3 e^{-i\omega\tau_2} \right) e^{-i\omega\tau_1} = 0.$$

In the similar way to analysis of τ_1, we can find critical values of τ_2 as

$$\tau_{2,m}^{\pm}(\omega) = \frac{1}{\omega}\left[\pm\psi_2(\omega) - \varphi_2(\omega) + 2m\pi\right] \tag{15}$$

where

$$
\begin{aligned}
A_2(\omega) &= \text{Re}\left[P_1\bar{P}_3 - P_0\bar{P}_2\right] = 0, \\
B_2(\omega) &= \text{Im}\left[P_1\bar{P}_3 - P_0\bar{P}_2\right] = k_2\omega\left[k_1^2(1 - \beta_1\beta_2) - \omega^2\right],
\end{aligned}
$$

$$\psi_2(\omega) = \cos^{-1}\left[\frac{|P_0|^2 - |P_1|^2 + |P_2|^2 - |P_3|^2}{2\sqrt{B_2(\omega)^2}}\right]$$

and

$$\varphi_2(\omega) = \arg\left[P_1\bar{P}_3 - P_0\bar{P}_2\right] = \begin{cases} \dfrac{\pi}{2} & \text{if } B_2(\omega) > 0, \\[2ex] \dfrac{3\pi}{2} & \text{if } B_2(\omega) < 0. \end{cases}$$

To define $\psi_2(\omega)$, we need a condition similar to $F(\omega) \leq 0$, that is,

$$G(\omega) = \left(|P_0|^2 - |P_1|^2 + |P_2|^2 - |P_3|^2\right)^2 - 4\left[B_2(\omega)\right]^2 \leq 0.$$

Since it can be shown that $F(\omega) = G(\omega)$, solutions of $F(\omega) = 0$ solve $G(\omega) = 0$. The results obtained so far are summarized as follows:

Theorem 2 *From (14) and (15), the following pair of delays*

$$\left\{(\tau_{1,m}^{\pm}(\omega),\ \tau_{2,n}^{\mp}(\omega)) \mid \omega \in \Omega\right\}$$

is the set of all crossing curves on the (τ_1, τ_2) plane for equations (4).

2.2 Identical Coefficients

We will consider the above-mentioned two cases further by performing numerical simulations to visualize the theoretical results obtained in Theorems 1 and 2. For this purpose, we make the following assumption of identical adjustment coefficients under which we examine Case I and then Case II.

Assumption 2. $k_1 = k_2 = k$

In Case I, an explicit form of τ_2^{ℓ} with $\ell = 0$ described by (11) is derived as follows. Applying Euler's formula to the left hand side of (10) and substituting P_i defined in (7) into the right hand side lead to

$$\cos\omega\tau_2 - i\sin\omega\tau_2 = \frac{\left(\omega^2 - k\omega\sin\omega\tau_1\right) - ik\omega\cos\omega\tau_1}{k^2(1 - \beta_1\beta_2)\cos\omega\tau_1 + i\left(k\omega - k^2(1 - \beta_1\beta_2)\sin\omega\tau_1\right)}. \tag{16}$$

Multiplying by conjugate of denominator, the new denominator becomes

$$D_1 = k^2\left[k^2(1 - \beta_1\beta_2)^2 - 2k\omega(1 - \beta_1\beta_2)\sin\omega\tau_1 + \omega^2\right].$$

8

The new numerator is denoted as $N_1 + iM_1$ with

$$N_1 = -(k\omega)^2 \beta_1 \beta_2 \cos \omega \tau_1$$

and

$$M_1 = -k\omega \left[k^2(1 - \beta_1 \beta_2) + \omega^2\right] + (k\omega)^2 (2 - \beta_1 \beta_2) \sin \omega \tau_1.$$

Comparing the left hand side of (16) with $N_1/D + iN_2/D$ yields

$$\cos \omega \tau_2 = \frac{N_1}{D_1} \text{ and } \sin \omega \tau_2 = -\frac{M_1}{D_1} \tag{17}$$

where the graphs of N_1/D_1 and $-M_1/D_1$ as functions of τ_1 are illustrated in Figure 1 for $\tau_1 \in [0, 2\pi]$ under the following benchmark parameter values given below in Assumption 3. These values are repeatedly used in the following numerical calculations. Each of the red N_1/D_1 curve and the blue $-M_1/D_1$ curve intersects the horizontal axis twice at the following points,

$$\tau_1^B \simeq 1.81, \ \tau_1^D \simeq 5.44 \text{ and } \tau_1^A \simeq 1.65, \ \tau_1^C \simeq 1.98.$$

We will refer to the dotted red curve later.

Assumption 3. $k = 1$, $\alpha_1 = \alpha_2 = 9$ and $\beta_1 = \beta_2 = 1/2$.
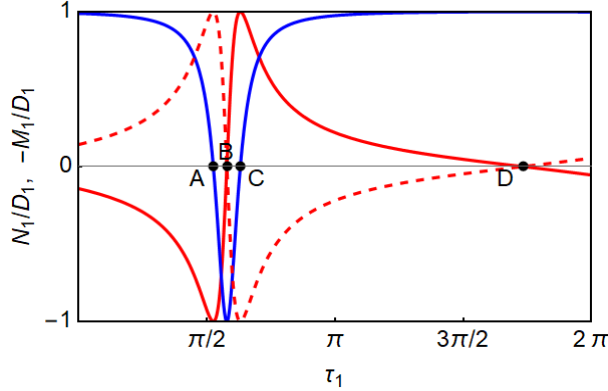

Figure 1. Graphs of N_1/D_1 (red) and $-M_1/D_1$
(blue)

It is observed that $\cos\omega\tau_2 < 0$ and $\sin\omega\tau_2 > 0$ for $\tau_1 \in (0, \tau_1^A)$. Hence solving $\cos\omega\tau_2 = N_1/D_1$ and $\sin\omega\tau_2 = -M_1/D_1$ for τ_2 yields

$$\tau_2^c(\tau_1) = \frac{1}{\omega} \cos^{-1}\left(\frac{N_1}{D_1}\right) \text{ and } \tau_2^s(\tau_1) = \frac{1}{\omega}\left[\pi - \sin^{-1}\left(-\frac{M_1}{D_1}\right)\right] \tag{18}$$

where the superscripts c and s stand for cos and sin, respectively. In the same way, $\cos \omega \tau_2 < 0$ and $\sin \omega \tau_2 < 0$ for $\tau_1 \in (\tau_1^A, \tau_1^B)$ that present

$$\tau_2^c(\tau_1) = \frac{1}{\omega}\left[2\pi - \cos^{-1}\left(\frac{N_1}{D_1}\right)\right] \text{ and } \tau_2^s(\tau_1) = \frac{1}{\omega}\left[\pi - \sin^{-1}\left(-\frac{M_1}{D_1}\right)\right]. \tag{19}$$

9

For $\tau_1 \in (\tau_1^B, \tau_1^C)$, $\cos\omega\tau_2 > 0$ and $\sin\omega\tau_2 < 0$ gives

$$\tau_2^c(\tau_1) = \frac{1}{\omega}\left[2\pi - \cos^{-1}\left(\frac{N_1}{D_1}\right)\right] \text{ and } \tau_2^s(\tau_1) = \frac{1}{\omega}\left[2\pi + \sin^{-1}\left(-\frac{M_1}{D_1}\right)\right]. \qquad (20)$$

Finally for $\tau_1 \in (\tau_1^C, \tau_1^D) \cup [\tau_1^D, 2\pi]$, $\cos\omega\tau_2 > 0$ and $\sin\omega\tau_2 > 0$ generate

$$\tau_2^c(\tau_1) = \frac{1}{\omega}\cos^{-1}\left(\frac{N_1}{D_1}\right) \text{ and } \tau_2^s(\tau_1) = \frac{1}{\omega}\sin^{-1}\left(-\frac{M_1}{D_1}\right). \qquad (21)$$

Since $\tau_2^s(\tau_1) = \tau_2^c(\tau_1)$ holds for any $\tau_1 \in [0, 2\pi]$, the solution can be denoted by $\tau_2(\tau_1)$.

The locus of $(\tau_1, \tau_2(\tau_1))$ for $\tau_1 \in [0, 2\pi]$ constructs the stability switching curve in Case I that is illustrated by two black curves in Figure 2. More precisely, the upper convex-shaped curve consists of three segments, each of which is described by (18), (19) and (20) whereas the lower concave-shaped curve is described only by (21).[1] It is numerically confirmed that the upper curve passes through point $\left(2\pi/3\sqrt{3}, 4\pi/3\sqrt{3}\right)$ at which the blue curve ends and the orange curve starts and that the lower curve passes through point $\left(4\pi/3\sqrt{3}, 2\pi/3\sqrt{3}\right)$ at which the green curve starts and the red curve ends.

In Case II with Assumption 2, solving $F(\omega) = 0$ yields simplified solutions,

$$\omega_1 = \omega_2 = k\sqrt{1 - \beta_1\beta_2}, \ \omega_3 = k(1 - \sqrt{\beta_1\beta_2}) \text{ and } \omega_4 = k(1 + \sqrt{\beta_1\beta_2}),$$

implying that

$$\Omega = [\omega_3, \omega_1] \cup [\omega_2, \omega_4].$$

Since $\omega_0 = \omega_i$ for $i = 1, 2$,

$$B_i(\omega) > 0 \text{ for } \omega \in [\omega_3, \omega_1) \text{ implying } \varphi_i(\omega) = \pi/2,$$
$$B_i(\omega) < 0 \text{ for } \omega \in (\omega_2, \omega_4] \text{ implying } \varphi_i(\omega) = 3\pi/2.$$

In Figure 2, the blue and red curves are described by the pairs of

$$\left(\tau_{1,0}^+(\omega), \ \tau_{2,1}^-(\omega)\right) \text{ and } \left(\tau_{1,1}^-(\omega), \ \tau_{1,0}^+(\omega)\right) \text{ for } \omega \in [\omega_3, \omega_1]$$

starting at point (π, π) for $\omega = \omega_3$. On the other hand, the green and orange curves are described by the pairs of

$$\left(\tau_{1,1}^+(\omega), \ \tau_{2,1}^-(\omega)\right) \text{ and } \left(\tau_{1,1}^-(\omega), \ \tau_{2,1}^+(\omega)\right) \text{ for } \omega \in [\omega_2, \omega_4]$$

ending at point $(\pi/3, \pi/3)$ for $\omega = \omega_4$. Hence the stationary point is stable in the lower-left region surrounded by the two black, orange and green curves. The hatched square is the region satisfying the HR conditions, (3). Notice that the square is inside the stable region we have just obtained. This is because HR derives one sufficient condition whereas we derive the sufficient and necessary condition. We will refer to the vertical dotted lines at $\tau_1 = \pi/3$ and $\tau_1 = 4\pi/3\sqrt{3}$ and points a, b, c later when we will perform numerical simulations.

Theorem 3 *The equilibrium point of dynamic system (4) is locally asymptotically stable for (τ_1, τ_2) in the region bounded by the stability switching curve that consists of the black, orange and green curves in the non-negative quadrant of (τ_1, τ_2).*

---

[1]It is, however, only some parts of the curves are illustrated for graphical simplicity.
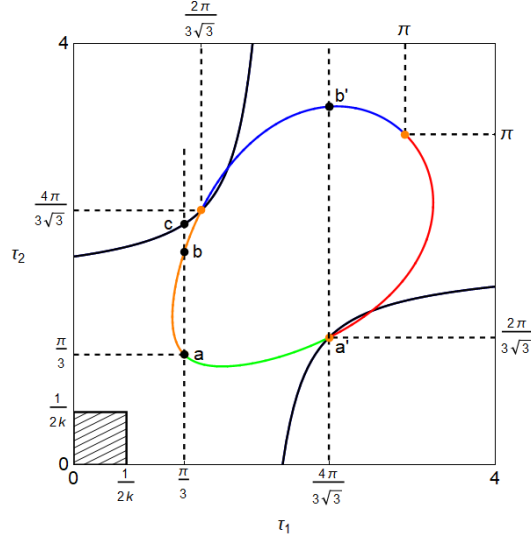
Figure 2. Division of the (τ_1, τ_2) plane

3 Delay Duopoly Model II

HR also examines the case where each firm has delayed information on its competitor's outputs but instantaneous knowledge of its own output. The homogenous system of the corresponding delay differential equations with $n = 2$ is

$$
\begin{aligned}
\frac{dx_1}{dt} &= k_1 \left[-x_1(t) - \beta_1 x_2(t - \tau_1) \right], \\
\\
\frac{dx_2}{dt} &= k_2 \left[-\beta_2 x_1(t - \tau_2) - x_2(t) \right],
\end{aligned}
\tag{22}
$$

where the non-diagonal variables are delayed. Its characteristic equation is

$$
\det \begin{pmatrix} \lambda + k_1 & k_1 \beta_1 e^{-\lambda \tau_1} \\ k_2 \beta_2 e^{-\lambda \tau_2} & \lambda + k_2 \end{pmatrix} = 0
$$

or

$$
\lambda^2 + k_1 k_2 + (k_1 + k_2)\lambda - k_1 k_2 \beta_1 \beta_2 e^{-\lambda \tau} = 0
\tag{23}
$$

where $\tau = \tau_1 + \tau_2 > 0$. Although the dynamic system (22) has two distinct delays, τ_1 and τ_2, it is essentially the same as a single delay system since only the value of the sum of these delays can affect dynamics. Suppose $\lambda = i\omega$ with $\omega > 0$ is a root of (23) for some τ and substitute it into (23) that can be separated to the real and imaginary parts,

$$
-\omega^2 + k_1 k_2 - k_1 k_2 \beta_1 \beta_2 \cos \omega \tau = 0,
$$

$$
(k_1 + k_2)\omega + k_1 k_2 \beta_1 \beta_2 \sin \omega \tau = 0.
$$

11

Moving the non-trigonometric terms to the right hand side and adding the squares of the two equations yield a quartic equation of ω

$$\omega^4 + \left(k_1^2 + k_2^2\right)\omega^2 + (k_1 k_2)^2 \left[1 - (\beta_1 \beta_2)^2\right] = 0$$

where the last term is positive due to Assumption 2. Positive coefficients of this equation imply no pure imaginary roots for equation (23). In other words, there are no roots of (23) that cross the imaginary axis when τ increases. Therefore no stability switch can occur, no matter how the delays are chosen. Such delays are called *harmless*. This is the same as the result shown by HR in a different way and can be summarized as follow.

Theorem 4 *The equilibrium point of dynamic system of* (22) *is locally asymptotically stable regardless of the values of* τ_1 *and* τ_2.

4 Delay Duopoly Model III

HR did not consider the case in which each firm has delayed knowledge of its own output but instantaneous knowledge of its competitors' outputs. In this section, we examine it where the dynamic system is constructed in the following way,

$$\frac{dx_1}{dt} = k_1\left[-x_1(t - \tau_1) - \beta_1 x_2(t)\right],$$

$$\frac{dx_2}{dt} = k_2\left[-\beta_2 x_1(t) - x_2(t - \tau_2)\right]$$

(24)

where the diagonal variables are delayed. With the same procedure above, we obtain the characteristic equation,

$$\det \begin{pmatrix} \lambda + k_1 e^{-\lambda \tau_1} & k_1 \beta_1 \\ \\ k_2 \beta_2 & \lambda + k_2 e^{-\lambda \tau_2} \end{pmatrix} = 0$$

that is equivalent to the equation

$$P_0(\lambda) + P_1(\lambda)e^{-\lambda \tau_1} + P_2(\lambda)e^{-\lambda \tau_2} + P_3(\lambda)e^{-\lambda(\tau_1 + \tau_2)} = 0$$

(25)

where

$$P_0(\lambda) = \lambda^2 - k_1 k_2 \beta_1 \beta_2, \ P_1(\lambda) = k_1 \lambda, \ P_2(\lambda) = k_2 \lambda, \ P_3(\lambda) = k_1 k_2.$$

Although each firm has a delay only in its own output, the characteristic equation (25) has the similar form to (6) in which each firm has not only the implementation delay on its own output but also the information delay on its competitor's output. Supposing $\lambda = i\omega$ with $\omega > 0$ and then following the same procedure as in Section 2, we have

$$|P_0(i\omega)|^2 + |P_1(i\omega)|^2 - |P_2(i\omega)|^2 - |P_3(i\omega)|^2 = 2A_1(\omega)\cos\omega\tau_1 - 2B_1(\omega)\sin\omega\tau_1$$

with

$$A_1(\omega) = \text{Re}\left[P_2(i\omega)\bar{P}_3(i\omega) - P_0(i\omega)\bar{P}_1(i\omega)\right] = 0,$$

$$B_1(\omega) = \text{Im}\left[P_2(i\omega)\bar{P}_3(i\omega) - P_0(i\omega)\bar{P}_1(i\omega)\right] = k_1\omega\left(k_2^2 - k_1 k_2 \beta_1 \beta_2 - \omega^2\right).$$

As before, we first consider the case of $A_1(\omega) = B_1(\omega) = 0$. It can be confirmed that $A_1(\omega) = 0$ always and $B_1(\omega) = 0$ holds for $\omega = \omega_0$ where

$$\omega_0^2 = k_2^2 - k_1 k_2 \beta_1 \beta_2.$$

On the other hand, $|P_0(i\omega)|^2 + |P_1(i\omega)|^2 - |P_2(i\omega)|^2 - |P_3(i\omega)|^2 = 0$ for $\omega = \omega_+$ where

$$\omega_+^2 = \frac{\left(k_2^2 - 2k_1 k_2 \beta_1 \beta_2 - k_1^2\right) + \sqrt{\left(k_2^2 - 2k_1 k_2 \beta_1 \beta_2 - k_1^2\right)^2 + 4\left(k_1 k_2\right)^2 \left[1 - (\beta_1 \beta_2)^2\right]}}{2}.$$

If $k_1 = k_2 = k$, then ω_0 and ω_+ are the same

$$\omega_0 = \omega_+ = k\sqrt{1 - \beta_1 \beta_2}$$

and this equality does not hold if $k_1 \neq k_2$. Hence, under the identical coefficient assumption, the stability switching curve is obtained as

$$e^{-i\omega_0 \tau_2} = -\frac{P_0(i\omega_0) + P_1(i\omega_0)e^{-i\omega_0 \tau_1}}{P_2(i\omega_0) + P_3(i\omega_0)e^{-i\omega_0 \tau_1}}. \tag{26}$$

As in the same analysis of Section 2.1, equation (26) can be rewritten as

$$\cos \omega_0 \tau_2 - i \sin \omega_0 \tau_2 = \frac{\left(\omega_0^2 + k^2 \beta_1 \beta_2 - k\omega_0 \sin \omega_0 \tau_1\right) - ik\omega_0 \cos \omega_0 \tau_1}{k^2 \cos \omega_0 \tau_1 + i\left(k\omega_0 - k^2 \sin \omega_0 \tau_1\right)}. \tag{27}$$

Multiplying conjugate of denominator to the denominator and numerator of the right hand side of (27) leads to the new denominator

$$D_3 = k^2 \left(k^2 - 2k\omega_0 \sin \omega_0 \tau_1 + \omega_0^2\right) \tag{28}$$

and the new numerator

$$N_3 + iM_3$$

where

$$N_3 = k^4 \beta_1 \beta_2 \cos \omega_0 \tau_1$$

and

$$M_3 = -k\omega_0 \left(k^2 + \omega_0^2 + k^2 \beta_1 \beta_2\right) + k^2 \left(2\omega_0^2 + k^2 \beta_1 \beta_2\right) \sin \omega_0 \tau_1.$$

Hence from the left hand side of (27) we have

$$\cos \omega_0 \tau_2 = \frac{N_3}{D_3} \text{ and } \sin \omega_0 \tau_2 = -\frac{M_3}{D_3} \tag{29}$$

where

$$\frac{N_3}{D_3} = \frac{k^2 \beta_1 \beta_2 \cos \omega_0 \tau_1}{k^2 - 2k\omega_0 \sin \omega_0 \tau_1 + \omega_0^2} = -\frac{N_1}{D_1}$$

and

$$\frac{M_3}{D_3} = \frac{-2k\omega_0 + \left(k^2 + \omega_0^2\right) \sin \omega_0 \tau_1}{k^2 - 2k\omega_0 \sin \omega_0 \tau_1 + \omega_0^2} = -\frac{M_1}{D_1}.$$

Comparing (29) with (17) reveals that in Figure 1, the M_3/D_3 curve is identical with the M_1/D_1 blue curve whereas the N_3/D_3 curve corresponds to the dotted red curve, that is, a horizontal-line mirror image of the N_1/D_1 red curve.

We now turn attention to the case of $[B_1(\omega)]^2 > 0$. As is shown above, we should have

$$F(\omega) = \left[|P_0|^2 + |P_1|^2 - |P_2|^2 - |P_3|^2\right]^2 - 4[B_1(\omega)]^2 \le 0$$

where $F(\omega)$ can be factored as

$$F(\omega) = F_a(\omega) \cdot F_b(\omega) \cdot F_c(\omega) \cdot F_d(\omega)$$

with

$$F_a(\omega) = \omega^2 + (k_1 + k_2)\omega + k_1 k_2 (1 + \beta_1 \beta_2),$$
$$F_b(\omega) = \omega^2 - (k_1 + k_2)\omega + k_1 k_2 (1 + \beta_1 \beta_2),$$
$$F_c(\omega) = \omega^2 + (k_1 - k_2)\omega - k_1 k_2 (1 - \beta_1 \beta_2),$$
$$F_d(\omega) = \omega^2 - (k_1 - k_2)\omega - k_1 k_2 (1 - \beta_1 \beta_2).$$

Solving each $F_i(\omega) = 0$ for $i = a, b, c, d$ yields two solutions and totally eight solutions are obtained,

$$\omega_\pm^a = \frac{k_1 + k_2 \pm \sqrt{(k_1 + k_2)^2 - 4k_1 k_2 (1 + \beta_1 \beta_2)}}{2} = k\left(1 \pm i\sqrt{\beta_1 \beta_2}\right),$$

$$\omega_\pm^b = \frac{-(k_1 + k_2) \pm \sqrt{(k_1 + k_2)^2 - 4k_1 k_2 (1 + \beta_1 \beta_2)}}{2} = k\left(-1 \pm i\sqrt{\beta_1 \beta_2}\right),$$

$$\omega_\pm^c = \frac{k_1 - k_2 \pm \sqrt{(k_1 - k_2)^2 + 4k_1 k_2 (1 - \beta_1 \beta_2)}}{2} = \pm k\sqrt{1 - \beta_1 \beta_2},$$

$$\omega_\pm^d = \frac{-(k_1 - k_2) \pm \sqrt{(k_2 - k_1)^2 + 4k_1 k_2 (1 - \beta_1 \beta_2)}}{2} = \pm k\sqrt{1 - \beta_1 \beta_2}.$$

Notice that the right most forms are obtained under the identical coefficient assumption. We see $F(\omega) > 0$ for $\omega \neq \omega_0$, implying no occurrence of the stability switch in the case of $[B_1(\omega)]^2 > 0$.

Returning to Figure 1 and (29), the stability switching curve with $B_1(\omega) = 0$ illustrated in Figure 3(A) is constructed as follows. Since $\cos \omega \tau_1 > 0$ and $\sin \omega \tau_1 > 0$ for $\tau_1 \in (0, \tau_1^A)$, we have

$$\tau_2^A(\tau_1) = \frac{1}{\omega_0} \cos^{-1}\left(\frac{N_3}{D_3}\right) \tag{30}$$

that describes the concave-shaped negative slope red curve in the lower-left corner. Since the stationary state is stable below the curve and unstable above, this is the stability switching curve on which the real part of an eigenvalue is zero, that is, stability is just lost. At $\tau_1 = \tau_1^A$, the corresponding value of τ_1 jumps up to the y-value of point A. Notice that HR's stability condition is satisfied in the small solid rectangular and is strictly below the curve. Since $\cos \omega \tau_2 > 0$ and $\sin \omega \tau_2 < 0$ for $\tau_1 \in (\tau_1^A, \tau_1^B)$ and $\cos \omega \tau_1 < 0$ and $\sin \omega \tau_1 < 0$ for $\tau_1 \in (\tau_1^B, \tau_1^C)$,

$$\tau_2^B(\tau_1) = \tau_2^C(\tau_1) = \frac{1}{\omega_0}\left[2\pi - \cos^{-1}\left(\frac{N_3}{D_3}\right)\right]$$

where $\tau_2^B(\tau_1)$ for $\tau_1 \in (\tau_1^A, \tau_1^B)$ describes the blue segment between A and B whereas $\tau_2^C(\tau_1)$ for $\tau_1 \in (\tau_1^B, \tau_1^C)$ describes the magenta segment between B and C. Further $\cos \omega \tau_1 < 0$ and $\sin \omega \tau_1 > 0$ for $\tau_1 \in (\tau_1^C, \tau_1^D)$ and $\cos \omega \tau_1 > 0$ and $\sin \omega \tau_1 > 0$ for $\tau_1 \in (\tau_1^D, 2\pi)$ presents the form of

$$\tau_2^D(\tau_1) = \tau_2^E(\tau_1) = \frac{1}{\omega_0} \cos^{-1}\left(\frac{N_3}{D_3}\right)$$

14

where $\tau_2^D(\tau_1)$ for $\tau_1 \in (\tau_1^C, \tau_1^D)$ describes the orange segment between C and D whereas $\tau_2^E(\tau_1)$ for $\tau_1 \in (\tau_1^D, 2\pi)$ describes the green segment between D and E. Finally,

$$\tau_2^{A'}(\tau_1) = \frac{1}{\omega_0}\left[\cos^{-1}\left(\frac{N_3}{D_3}\right) + 2\pi\right]$$

describes the red segment that shifts the $\tau_2^A(\tau_1)$ curve upward with 2π and the right most red curve is described by $\tau_2^A(\tau_1)$ for $\tau_1 \in (2\pi, 9.80)$. It is to be notice that the y-value of point E is $\tau_2^E = \tau_2^A(2\pi)$. On the winding downward-sloping curve located above-rightward of the stability switching curve, one of the eigenvalues is purely imaginary but the stability is already unstable there and no stability switch occurs.

Theorem 5 *The stability switching curve of dynamic system* (24) *is described by*

$$\tau_2^A(\tau_1) = \frac{1}{\omega_0}\cos^{-1}\left(\frac{N_3}{D_3}\right) \text{ for } \tau_1 \in (0, \tau_1^A).$$

To compare the stability switching curve of Model I with that of Model III, we enlarge the lower-left corner of Figure 3(A) and put the red stability switching curve (30) on the black stability switching curve of Model I in Figure 3(B). Due to the different shapes of these two curves, the region of (τ_1, τ_2) is divided into five subregions. Both models are stable in region labelled by $[S]$ and unstable in region $[U]$ indicating that roughly speaking, the delays become destabilizers when their lengths are relatively large and do not affect stability when they are smaller. Although Theorem 4 implies that the information delays are harmless to stability if the dynamic process involves only these, the division in Figure 3(B) reveals a different role of the information delay. In region $[A]$, Model I with information delays is unstable and Model III with no information delays is stable, implying that the information delays destabilize Model I when τ_1 and τ_2 are *symmetry* in the sense that they have the similar values. On the other hand, in regions $[B_1]$ and $[B_2]$, Model I is stable and Model III is unstable, implying that the information delays stabilize Model I when τ_1 and τ_2 are *asymmetry* in the sense that one of them takes a larger value and the other a smaller value. We summarize these results as follows:

Proposition 1 *When a dynamic system has both of the implementation and information delays, the information delays can change its role to stabilizer from destabilizer when the delays become asymmetry from symmetry.*
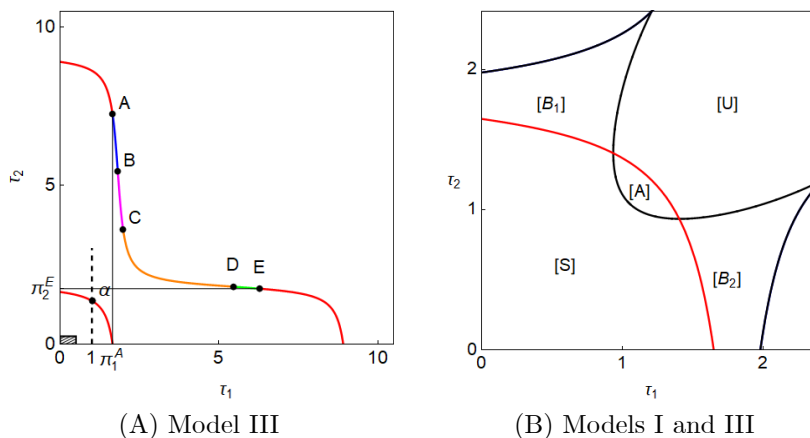

(A) Model III   (B) Models I and III

Figure 3. Stability switching curves

15

5 Numerical Simulations

So far we have imposed the identical coefficient assumption of $k_1 = k_2$ on the output adjustment process and confine attention to a small neighborhood of the equilibrium point. In this section we modify the dynamic equations and numerically confirm the theoretical results obtained. To this end, we first introduce some nonlinearities into Models I and III to examine global behavior. Second, we take away the identical assumption (i.e., Assumption 2) and then consider how the non-identical coefficients affect the shape of the stability switching curves and the resultant dynamics.

5.1 Global Dynamics

Since the corresponding nonhomogenous systems of (4) and (24) are still linear, trajectories generated by these systems are divergent when the systems are locally unstable. To avoid such uninteresting and unrealistic dynamics, we introduce some nonlinearities and see the effects caused by the delays on global dynamics. The nonlinearity that we consider comes from an idea of a flexible adjustment, that is, the output adjustment responds positively to the gap between the optimal and actual outputs and the degree of responsiveness depends on the level of output in the following way,

$$K_i(x_i) = k_i \left[a_2 \left(\frac{a_1 + a_2}{a_1 e^{-(x_i - x_i^*)} + a_2} - 1 \right) + 1 \right].$$

It can be checked that

$$K_i(x_i^*) = k_i, \ \lim_{x_i \to \infty} K_i(x_i) = k_i (1 + a_1) \text{ and } K_i(0) = k_i \left[\frac{a_2 (a_1 + a_2)}{a_1 e^{x_i^*} + a_2} + 1 - a_2 \right] > 0$$

where $a_1 = 1$ and $a_2 = 1$ are assumed in the following numerical simulations.

Model I is now nonlinearized as

$$\frac{dx_1}{dt} = K_1 [x_1(t)] [-x_1(t - \tau_1) - \beta_1 x_2(t - \tau_1) + \alpha_1],$$

$$\frac{dx_2}{dt} = K_2 [x_2(t)] [-\beta_2 x_1(t - \tau_2) - x_2(t - \tau_2) + \alpha_2],$$

(31)

both of which can be reduced to (4) by linear approximation in the neighborhood of the equilibrium point. We perform two simulations. In the first simulation, we choose τ_2 as a bifurcation parameter and increase the value of τ_2 from 0 to 5 with an increment of 0.01 along the vertical dotted line at $\tau_1 = \pi/3 \simeq 1.05$ in Figure 2. For each value of τ_2, the fully delayed system (31) is simulated for $0 \le t \le 1000$. We generate 1000 data of $x_2(t)$ from the solutions for $t \in [900, 1000]$ by changing t with an increment of 0.1 and then plot the local maximum and minimum out of the data vertically just above the point τ_2, to illustrate the corresponding bifurcation diagram with respect to τ_2 in Figure 4(A). The vertical line at $\tau_1 = \pi/3$ passes through the point at which the orange and green curve are connected (i.e., $\tau_2^a = \pi/3$), crosses the orange curve at $\tau_2^b \simeq 2.02$ and then crosses the black curve at $\tau_2^b \simeq 2.28$. Figure 4(A) indicates that the equilibrium point is stable for $\tau_2 < \tau_2^a$ and loses stability at the first intersection at point $a = (\pi/3, \tau_2^a)$. The equilibrium point bifurcates to a limit cycle for $\tau_2 \in (\tau_2^a, \tau_2^b)$ and then regains stability when it arrives at the second intersection $(\pi/3, \tau_2^b)$.[2] For further increases of τ_2 the system loses stability again at $(\pi/3, \tau_2^c)$ and the corresponding bifurcation gets a bit complicated.

---

[2] It is possible to determine directions of the stability switch analytically. See Lin and Wang (2012) for theoretical base and Matsumoto and Szidarovszky (2015) for its application.

In particular, a limit cycle with two extremum (one maximal and one minimal) emerges first and then it turns to be a cycle with four extremum that then becomes the one with six extremum and so on. The system does not regain stability for values of τ_2 larger than τ_2^c.

In the second simulation, we change the value of τ_1 to $4\pi/3\sqrt{3} \simeq 2.42$ and repeat the same procedure to obtain the bifurcation diagram illustrated in Figure 4(B). The starting point $(4\pi/3\sqrt{3}, 0)$ is located in the region to the right of the lower black curve in Figure 2, the equilibrium point is locally unstable and Figure 4(B) indicates the birth of a limit cycle at this point. As the value of τ_2 increases along the vertical dotted line at $\tau_1 = 4\pi/3\sqrt{3}$, the corresponding limit cycle gradually shrinks and discontinuously jumps to a different limit cycle at point $(4\pi/3\sqrt{3}, \tau_2^a)$ where $\tau_2^a = 2\pi/3\sqrt{3} \simeq 1.21$. Further increasing τ_2 leads to complicated dynamics through ála period-doubling cascade. Notice that τ_i has exactly the same effect as τ_j as the stability switching curve is symmetric with respect to the diagonal. These numerical results are summarized as follow.

Proposition 2 *In the dynamic process of nonlinearized Model I, (1) the delay has the dual roles of destabilizer and stabilizer according to its length when the stationary state is locally stable at the starting point and (2) increasing a value of delay can generate complex dynamics involving chaotic behavior when the stationary state is locally unstable at the starting point.*
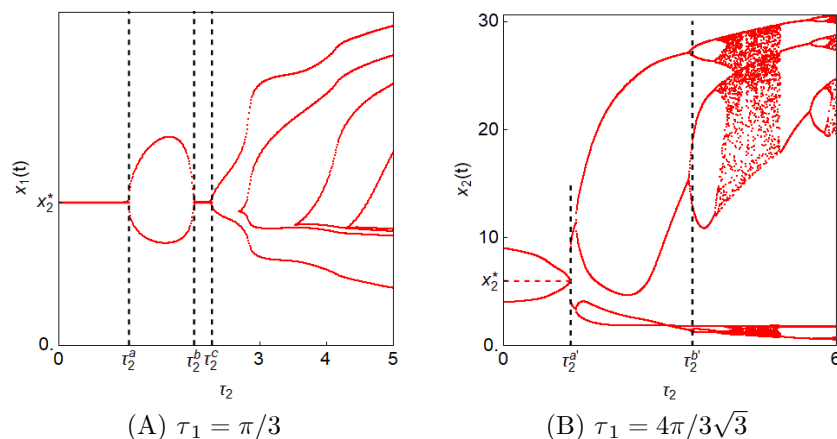

(A) $\tau_1 = \pi/3$ (B) $\tau_1 = 4\pi/3\sqrt{3}$

Figure 4. Bifurcation diagrams of the nonlinear Model I

We now turn attention to the nonlinearized Model III,

$$\frac{dx_1}{dt} = K_1\left[x_1(t)\right]\left[-x_1(t-\tau_1) - \beta_1 x_2(t) + \alpha_1\right],$$

$$\frac{dx_2}{dt} = K_2\left[x_2(t)\right]\left[-\beta_2 x_1(t) - x_2(t-\tau_2) + \alpha_2\right].$$

Two simulations are performed for the new Model III.[3] The first simulation is presented in Figure 5(A) in which the value of τ_2 increases from 0 to 3 along the vertical dotted line at $\tau_1 = 1$ in

---

[3]Matsumoto and Szidarovszky (2015) also consider dynamics of a delay nonlinear model of Cournot duopoly having the similar structure. However the growth rate of outputs is determined by a product of the marginal profit and an adjustment function depending on the level of output. As a natural consequence of the different adjustment process, it has different dynamic behavior.

Figure 3(A). The system is asymptotically stable for the starting point of $\tau_1 = 1$ and $\tau_2 = 0$ and remains stable until point $(1, \tau_2^A)$ where point a is on the stability switching curve in Figure 3(A). As is seen, at a critical value τ_2^A, the stationary state loses stability and bifurcates to a limit cycle. Notice that the stability regain does not occur and thus the delay does not have the dual roles. As seen in Figure 4(A), making τ_2 larger than the critical value of τ_2^A increases the number of extremum of the limit cycle. In the second simulation, we change the fixed value of τ_1 to 2 and repeat the same procedure. However, to avoid graphical congestion of Figure 3(A), the line at $\tau_1 = 2$ is not illustrated. The resultant dynamics illustrated in Figure 5(B) in which the system is unstable and its dynamic behavior gets complicated as τ_2 increases, that is, we alternatively have windows for complex dynamics and the one for a periodic limit cycle.

Proposition 3 *In the dynamic process of nonlinearized Model III, (1) stability is lost at $\tau_2 = \tau_2^A$ and never regained since the delay crosses the stability switching curves only once when the stationary state is stable at the starting point; (2) as τ_2 increases, dynamics alternates between complicated behavior and periodic cyclic behavior with increasing the periodic number.*

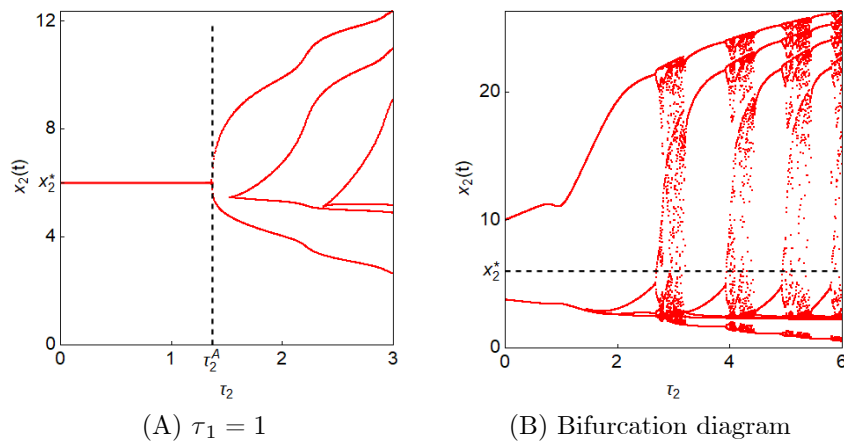(A) $\tau_1 = 1$ (B) Bifurcation diagram

Figure 5. Bifurcation diagrams of the nonlinear Model III

5.2   Non-Identical Coefficients

We now use the non-identical adjustment coefficients to see how such asymmetry affects the results obtained. We have already shown that the stability switching curves in Case I (that is, the black curves in Figure 2) can be constructed only under Assumption 2. It is expected that the stability switching curves obtained in Case II may be distorted. In order to illustrate the non-identical effects, we present numerical simulations concerning the shape of the stability switching curves and the dynamics of the nonlinearized Model I. The values of the coefficients are $k_1 = 3/2$ and $k_2 = 1$ in the first simulation and are changed to $k_1 = 1/2$ and $k_2 = 1$ in the second.

In the first simulation, solving $F(\omega) = 0$ determines the interval $\Omega = [\omega_3, \omega_1] \cup [\omega_2, \omega_4]$ where

$$\omega_3 \simeq 0.589, \quad \omega_1 \simeq 0.840, \quad \omega_2 \simeq 1.340, \quad \omega_4 \simeq 1.911.$$

Notice that $\omega_1 \neq \omega_2$ when $k_1 \neq k_2$. In Figure 6(A) stability switching curves are illustrated as solid curves in the same color as in Figure 2, that is, the blue curve is described

by $\left(\tau_{1,0}^+(\omega),\ \tau_{2,1}^-(\omega)\right)$ for $\omega \in [\omega_3, \omega_1]$ and the red curve exists outside the designated region whereas the green and orange curves are given by $\left(\tau_{1,1}^+(\omega),\ \tau_{2,1}^-(\omega)\right)$ and $\left(\tau_{1,1}^-(\omega),\ \tau_{2,1}^+(\omega)\right)$ for $\omega \in [\omega_2, \omega_4]$ and they end at the same point $(\tau_1^*(\omega_4), \tau_2^*(\omega_4))$.[4] The nonlinear system (31) is asymptotically stable in the lower-left region surrounded by these curves. It is seen that the shaded rectangular, HR's stability region, is still inside it. The stability switching curves with $k_1 = k_2 = 1$ are also illustrated as the dotted curves in the same color. Comparing the new stability region with the old one reveals that the asymmetric coefficients shift the solid orange curve leftward and the solid green curve downward, resulting in a shrink of the stability region. On the other hand, a part of the solid blue curve is located above the dotted black curve, indicating an enlargement of the stability region. As far as the current example is concerned, the increase seems to be larger than the decrease. Thus the stability region becomes smaller. It is not sure if this result is specific or general. The bifurcation diagram with respect to τ_2 in Figure 6(B) is constructed along the vertical dotted line at $\tau_1 = \tau_1^*(\omega_4)$. The vertical line intersects these stability switching curves three times at the following values of τ_2,

$$\tau_2^a \simeq 0.822,\ \tau_2^b \simeq 1.325 \text{ and } \tau_2^c \simeq 2.36$$

which are at the connecting point of the green and orange curves, on the orange curve and on the blue curve, respectively. Stability is lost at $\tau_2 = \tau_2^a$ and regained at $\tau_2 = \tau_2^b$ while a limit cycle is born for $\tau_2 \in (\tau_2^a, \tau_2^b)$. Stability is lost again at $\tau_2 = \tau_2^c$ and not regained for any $\tau_2 > \tau_2^c$. The diagram indicates that a limit cycle becomes more distorted as the value of τ_2 is getting larger.

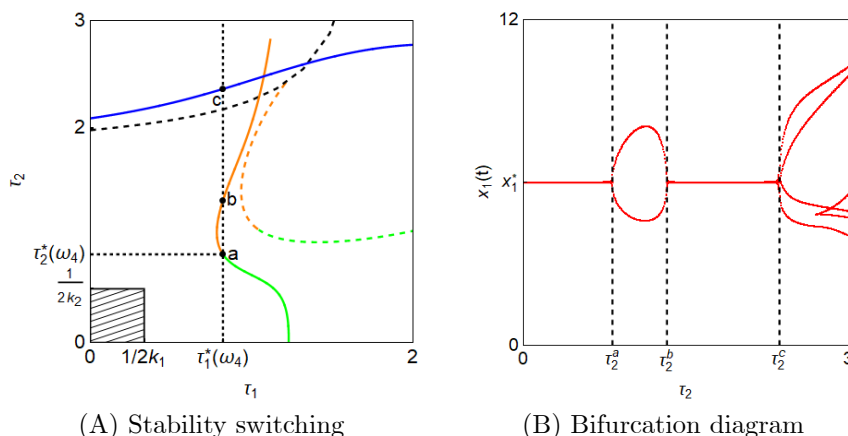(A) Stability switching   (B) Bifurcation diagram

Figure 6. $k_1 = 1.5$ and $k_2 = 1$

In the second simulation, the different value of k_1 presents different solutions for $F(\omega) = 0$,

$$\omega_3 \simeq 0.317,\ \omega_1 \simeq 0.411,\ \omega_2 \simeq 0.911,\ \omega_4 \simeq 1.183.$$

In Figure 7(A) the red curve is described by $\left(\tau_{1,1}^-(\omega),\ \tau_{1,0}^+(\omega)\right)$ for $\omega \in [\omega_3, \omega_1]$ and the region surrounded by the orange, green and red curves is the stability region that includes the shaded rectangular region. As in Figure 6(A), the stability switching curves with $k_1 = k_2 = 1$ are illustrated as the dotted curves in the same color. It is seen that decreasing the value of k_1 shifts the solid green curve upward and makes the slope of the solid orange curve flatter. As

---

[4]Needless to say, $\tau_1^*(\omega_4) = \tau_{1,1}^+(\omega_4) = \tau_{1,1}^-(\omega_4)$ and $\tau_2^*(\omega_4) = \tau_{2,1}^-(\omega_4) = \tau_{2,1}^+(\omega_4)$.

a result, the stability region is increased in one part and decreased in the other part. In the current example, the stability region becomes larger. The bifurcation diagram with respect to τ_1 in Figure 7(B) illustrates the change of dynamical behavior of the nonlinearized Model I as the length of the delay τ_1 is varied along the horizontal dotted line at $\tau_2 = \tau_2^*(\omega_4)$. It is observed that the bifurcation diagram in Figure 7(B) is similar to the diagrams in 6(B). In particular, stability is lost at $\tau_1 = \tau_1^a$ and regained at $\tau_1 = \tau_1^b$ whereas a limit cycle emerges for $\tau_1 \in (\tau_1^a, \tau_1^b)$. It is lost again at $\tau_1 = \tau_1^c$. and never regained for any $\tau_1 > \tau_1^c$. A limit cycle emerges for $\tau_1 > \tau_1^c$ and becomes larger with increasing the number of the extrema as τ_1 gets larger than τ_1^c.

We summarize the effect caused by asymmetry coefficients.

Proposition 4 *Non-identical coefficients of k_1 and k_2 distort the shape of the stability switching curve and it depends on the relative magnitude of the coefficients whether the stability region becomes larger or smaller.*
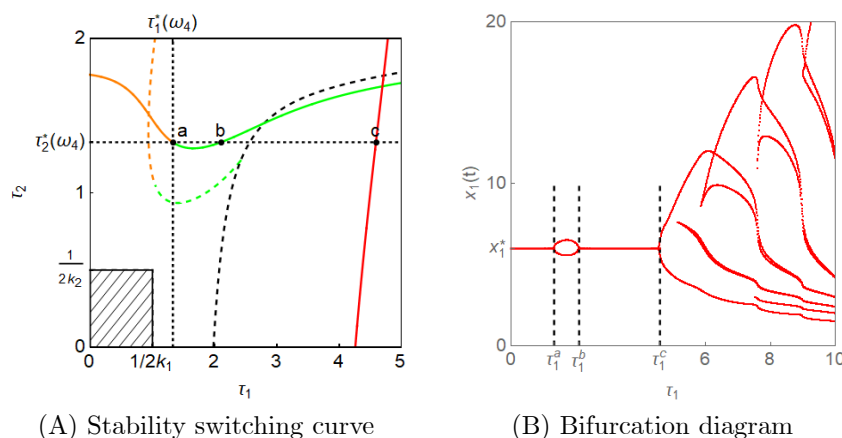

(A) Stability switching curve   (B) Bifurcation diagram

Figure 7. $k_1 = 0.5$ and $k_2 = 1$

6 Concluding Remarks

In this paper we have analyzed the dynamics of three different types of the Cournot duopoly model with multiple discrete delays, Model I with the implementation and information delays, Model II with only the information delays and Model III only with the implementation delays. For stability analysis, we adopted the linear models that were used by HR and constructed the stability switching curve on which stability was lost or gained. For global dynamics, we nonlinearized the models and performed numerical simulations. In doing so, we demonstrated three main results:

(i) In Model I, the delays has the dual roles of destabilizer and stabilizer and complicated dynamics involving chaotic behavior can emerge for larger values of the delays.

(ii) In Model II, the information delays alone do not affect stability.

(iii) In Model III, the implementation delays can destabilize the otherwise stable stationary state, however, they do not have the dual roles.

References

[1] Bischi, G. I., Chiarella, C., Kopel, M. and Szidarovszky, F., *Nonlinear oligopolies: stability and bifurcations*, Heidelberg Dordrecht, London, New York, Springer 2010.

[2] Cooke, K. L. and Grossman, Z., Discrete delay, distributed delay and stability switches, *Journal of Mathematical Analysis and Applications*, 86, 592-627, 1982.

[3] Cournot, A., *Recherches sur les Principes Mathématiques de la Théorie des Richessess*, Paris, Hachette, 1838 (Englich translation: *Researches into the mathematical principles of the theory of wealth*, New York, Kelley, 1960).

[4] Fisher, F., The stability of the Cournot solution: the effects of speeds of adjustment and increasing marginal costs, *Review of Economic Studies*, 28, 125-135, 1961.

[5] Gori, L, Guerrini, L. and Sodini, M., A continuous time Cournot duopoly with delays, *Chaos, Solitons and Fractals*, 79, 166-177, 2015.

[6] Gu, K., Niculescu, S. and Chen, J., On stability crossing curves for general systems with two delays, *Journal of Mathematical Analysis and Applications*, 311, 231-252, 2005.

[7] Hahn, F., The stability of the Cournot oligopoly solution, *Review of Economic Studies*, 29, 329-331, 1962.

[8] Howroyd, T. D. and Russel, A. M., Cournot oligopoly models with time delays, *Journal of Mathematical Economics,* 13, 97-108, 1984.

[9] Lin, X. and Wang, H., Stability analysis of delay differential equations with two discrete delays, *Canadian Applied Mathematics Quarterly*, 20, 519-133, 2012.

[10] McManus, M. and Quandt, R., Equilibrium numbers and size in Cournot oligopoly, *Yorkshire Bulletin of Social Science and Economic Research*, 16, 68-75, 1964.

[11] Matsumoto, A. and Szidarovszky, F., Nonlinear Cournot duopoly with implementation delays, *Chaos, Solitions and Fractals*, 79, 157-165, 2015.

[12] Okuguchi, K., *Expectations and stability in oligopoly models*, Berlin, Springer, 1976.

[13] Okuguchi, K. and Szidarovszky, F., *The theory of oligopoly with multi-product firms*, 2nd edition, Berlin, Springer, 1999.

[14] Theocharis, R. D., On the stability of the Cournot solution on the oligopoly problem, *Review of Economic Studies*, 27, 133-134, 1960.